

# ChemComm

Accepted Manuscript



This is an *Accepted Manuscript*, which has been through the Royal Society of Chemistry peer review process and has been accepted for publication.

*Accepted Manuscripts* are published online shortly after acceptance, before technical editing, formatting and proof reading. Using this free service, authors can make their results available to the community, in citable form, before we publish the edited article. We will replace this *Accepted Manuscript* with the edited and formatted *Advance Article* as soon as it is available.

You can find more information about *Accepted Manuscripts* in the [Information for Authors](#).

Please note that technical editing may introduce minor changes to the text and/or graphics, which may alter content. The journal's standard [Terms & Conditions](#) and the [Ethical guidelines](#) still apply. In no event shall the Royal Society of Chemistry be held responsible for any errors or omissions in this *Accepted Manuscript* or any consequences arising from the use of any information it contains.

## COMMUNICATION

# A narrow-bandgap benzobisthiadiazole derivative with high near-infrared photothermal conversion efficiency and robust photostability for cancer therapy

Cite this: DOI: 10.1039/x0xx00000x

Received 00th January 2012,  
Accepted 00th January 2012

DOI: 10.1039/x0xx00000x

www.rsc.org/

Shuo Huang,<sup>a</sup> Ravi Kumar Kannadorai,<sup>a</sup> Yuan Chen,<sup>a</sup> Quan Liu,<sup>a,\*</sup> Mingfeng Wang<sup>a</sup>

Photothermal therapy has emerged as a promising tool for treatment of diseases such as cancers. Previous photothermal agents have been largely limited to inorganic nanomaterials and conductive polymers that are barely biodegradable, thus raising issues of long-term toxicity for clinical applications. Here we report a new photothermal agent based on colloidal nanoparticles formed by a small-molecular dye, benzo[1,2-c;4,5-c']bis[1,2,5]thiadiazole-4,7-bis (5-(2-ethylhexyl)thiophene). These nanoparticles showed strong near-infrared absorption, robust photostability and high therapeutic efficiency for photothermal treatment of cancer cells.

As one of major causes of death, cancer and malignant tumors have greatly threatened human health. Photothermal therapy (PTT) that converts absorbed light energy into heat has attracted great attention due to many advantages, such as high specificity, minimal invasiveness, low toxicity to normal tissues, and excellent anti-cancer efficacy.<sup>1-3</sup> For the *in vivo* applications of PTT, therapeutic agents with strong optical absorbance in the near-infrared (NIR) therapeutic optical window (700-1000 nm) are preferable to minimize light attenuation in tissues in order to achieve a maximal light penetration depth. Moreover, biological chromophores will be affected minimally in this region.<sup>4</sup> The localization of laser energy for determining the heating profile and subsequent PTT effect can also be simulated beforehand.<sup>5,6</sup> In addition, the agents used for PTT should be biocompatible and non-toxic. In recent years, a variety of NIR-absorbing inorganic nanomaterials, such as gold nanostructures,<sup>7-12</sup> Pd nanosheets,<sup>13</sup> carbon nanomaterials,<sup>14,15</sup> rare earth ions doped nanocrystals,<sup>16</sup> copper sulfide nanoparticles,<sup>17,18</sup> tungsten oxide nanowires,<sup>19</sup> quantum dots<sup>20</sup> and porous silicon<sup>21</sup> have been explored for PTT. Although the high efficacy for PTT treatment of cancers has been demonstrated using most of

these inorganic nanomaterials, they are non-biodegradable and tend to retain in the body for a long period of time, raising the issue of long-term toxicity in potential clinical applications.<sup>22</sup>

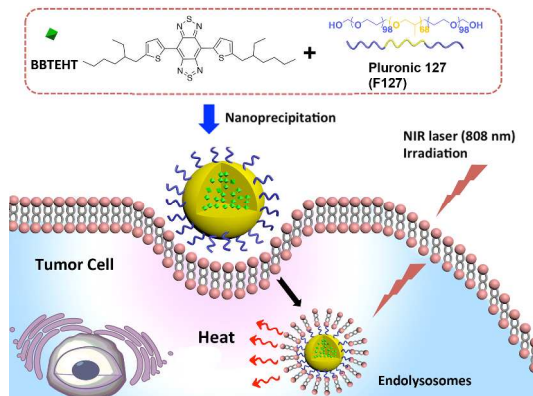
As a consequence, photothermal agents based on organic NIR-absorbing materials have attracted increasing attention recently. For instance, NIR-absorbing agents based on conjugated polymers with appropriate aromatic structures, such as polyaniline, poly-(3,4-ethylenedioxythiophene):poly(4-styrenesulfonate)(PEDOT:PSS), polypyrrole, and dopamine-melanin exhibit high photothermal conversion efficacy in PTT-based cancer treatment.<sup>23-26</sup> Despite the encouraging PTT therapeutic effects obtained from those polymeric nanoparticles, the biodegradation behavior of conjugated polymers remains unclear.

On the other hand, small molecular organic dyes such as indocyanine green (ICG)<sup>27,28</sup> and methylene blue<sup>29</sup> have been used not only in fluorescence-based imaging, but also as PTT agents. These small molecular PTT agents show advantages such as their well-defined molecular structures, good synthetic reproducibility in contrast to the batch-to-batch difference in polymer synthesis, and the potentially improved biodegradability. The further exploration of these small molecular PTT agents, nevertheless, is limited by their poor photostability and short circulation time.<sup>30</sup> Recently, a synthetic heptamethine indocyanine dye encapsulated by PEG-grafted poly(maleicanhydride-alt-1-octadecene) showed improved photostability than ICG and has been used as a photothermal agent for *in vivo* cancer therapy.<sup>27</sup> Other nanoparticles (NPs), for example, formed by self-assembly of porphyrin-lipid conjugates have been recently reported as a new type of PTT agent.<sup>31</sup>

Herein, we report a new photothermal agent based on a small-molecular dye, benzo[1,2-c;4,5-c']bis[1,2,5]thiadiazole-4,7-bis (5-(2-ethylhexyl)thiophene) (BBTEHT). BBT unit, due to its hypervalent sulfur atoms stabilized in quinoidal structures in a conjugated backbone, is a strong electron accepting unit that

ensures strong NIR absorption of BBTEHT in the therapeutic optical window.<sup>32-38</sup> The NPs formed by BBTEHT molecules were prepared through nanoprecipitation in the presence of Pluronic<sup>®</sup> 127 as the stabilizer, which is commercially available and has been widely used to encapsulate hydrophobic therapeutic agents for drug delivery.<sup>39, 40</sup> Under 808-nm NIR laser irradiation, BBTEHT NPs showed improved photostability and higher photothermal conversion efficacy compared to that of commercial gold (Au) nanorods. In addition, BBTEHT NPs at a concentration as low as 35  $\mu\text{g}/\text{mL}$  achieved an excellent therapeutic efficacy with nearly 100% cancer cell death.

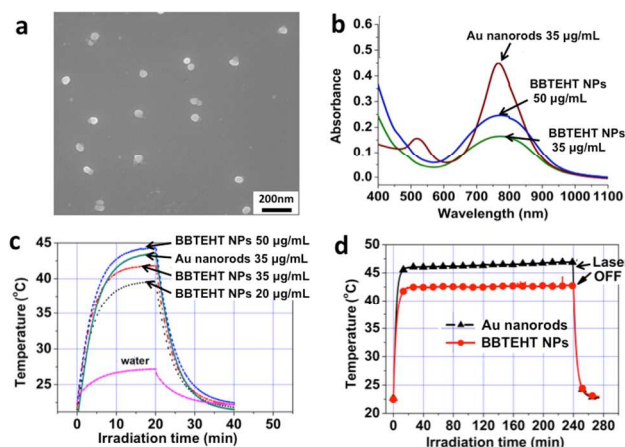
BBTEHT was synthesized following a procedure<sup>41</sup> described in the Supplementary Information. The chemical structure of BBTEHT was confirmed by <sup>1</sup>H-NMR (Fig. S1), <sup>13</sup>C-NMR (Fig. S2), melting point, FTIR and MALDI-TOF mass spectroscopy (Fig. S4). BBTEHT as a narrow-bandgap molecule showed two absorption peaks in an organic solvent such as toluene, one around 350 nm and the other at 770 nm, with an onset around 900 nm (Fig. S3). The calculated molar absorption coefficient of BBTEHT at the peak of 770 nm was  $2.6 \times 10^4 \text{ L} \cdot \text{mol}^{-1} \cdot \text{cm}^{-1}$ . The absorption spectrum appeared slightly broader after BBTEHT molecules were encapsulated with Pluronic<sup>®</sup> 127 and dispersed in water (Fig. 1b).



**Scheme 1.** Schematic illustration of the preparation of BBTEHT nanoparticles via nanoprecipitation process in the presence of Pluronic<sup>®</sup> 127 as the stabilizer.

Scheme 1 shows the molecular structure of BBTEHT and a schematic presentation of the NPs formed through a nanoprecipitation process.<sup>42</sup> More experimental details of the NP preparation are described in the Supplementary Information. At a concentration (e.g. 8.3 mg/mL) above the critical micelle concentration (CMC) of Pluronic<sup>®</sup> 127 in water,<sup>40</sup> self-assembly is driven by the hydrophobic interaction between the polypropylene oxide (PPO) block of Pluronic<sup>®</sup> 127 and BBTEHT which collapses to form the core of the NPs. The shell of the NPs consists of PEG chains originated from Pluronic<sup>®</sup> 127 that extrude to the aqueous media to provide the colloidal stability.

A representative scanning electron microscopy (SEM) image (Fig. 1a) shows that the resulting spherical particles appear uniform in size and shape, although a small population of tiny NPs can also be observed in both transmission electron microscopy (TEM) (Fig. S5a) and SEM images. A statistical analysis of the particle size gives an average diameter of  $53 \pm 9$  nm. In addition, the size and shape of the NPs measured with TEM (Fig. S5a) are consistent with those measured with SEM.



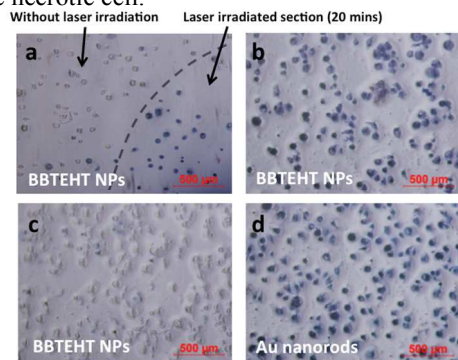
**Fig. 1** a) SEM image of BBTEHT NPs from a dispersion of 35  $\mu\text{g}/\text{mL}$ . b) UV-Vis-NIR spectra of BBTEHT NPs (35 and 50  $\mu\text{g}/\text{mL}$ , respectively) and Au nanorods (35  $\mu\text{g}/\text{mL}$ ). c) Temperature change plots of different concentration BBTEHT NPs and Au nanorods under irradiation by an 808-nm laser with a power density of 1.77  $\text{W}/\text{cm}^2$  for 20 mins. d) Temperature elevation of BBTEHT NPs and Au nanorods both at a concentration of 35  $\mu\text{g}/\text{mL}$  under irradiation of laser (808 nm, 1.77  $\text{W}/\text{cm}^2$ ) for 4 h. All of the concentrations of the BBTEHT NPs are calculated based on the mass of BBTEHT without inclusion of the stabilizer (i.e. Pluronic<sup>®</sup> 127).

Fig. 1c-d shows the photothermal efficiency and photostability of BBTEHT NPs in comparison with commercially available Au nanorods with NIR absorption similar to that of BBTEHT NPs (Fig. 1b). The photothermal effect induced by NIR laser illumination at 808 nm with a power density of 1.77  $\text{W}/\text{cm}^2$  for 20 mins in the presence of BBTEHT NPs was investigated by monitoring the temperature of 1 mL aqueous dispersion of BBTEHT NPs at various concentrations (20, 35, and 50  $\mu\text{g}/\text{mL}$ ). Obvious concentration dependence was observed under laser irradiation of the aqueous dispersions containing BBTEHT NPs, whereas pure water as a control showed little change in temperature under the same conditions of laser irradiation. As shown in Fig. 1c, the temperature of BBTEHT NPs and Au nanorods with the same mass concentration (35  $\mu\text{g}/\text{mL}$ ) increased to 42.0 and 43.6  $^{\circ}\text{C}$ , respectively, which fell within the hyperthermia region (41-47  $^{\circ}\text{C}$ )<sup>43</sup>. The slightly less temperature rise of BBTEHT NPs compared to that of Au nanorods could be attributed to the lower optical density at 808 nm of BBTEHT NPs compared to Au nanorods (Fig. 1c). These results indicate that BBTEHT NPs could act as an efficient photothermal agent, with photothermal conversion efficiency even higher than that of Au nanorods if their optical densities are matched.

When the NIR laser irradiation time was extended up to 4 h, the temperature of both Au nanorods and BBTEHT NPs at the same concentration of 35  $\mu\text{g}/\text{mL}$  reached a plateau at the level of 45-46  $^{\circ}\text{C}$  and 42-43  $^{\circ}\text{C}$ , respectively (Fig. 1d). In addition, there was no obvious change of the maximum absorption peak in the NP dispersion after irradiation compared to the NPs before irradiation (Fig. S5b). Nevertheless, both the SEM and the TEM images (Fig. S5c and d) of BBTEHT NPs after laser irradiation show some agglomeration of the NPs, which could be due to the thermally induced gelation behavior of Pluronic<sup>®</sup> 127.<sup>44-47</sup>

To evaluate the hyperthermic effect of BBTEHT NPs on human renal cell carcinoma, caki-2 cell lines were prepared in a 24-well plate following a procedure described in the Supplementary Information. The NPs were uptaken by cells likely through receptor-mediated endocytosis (RME).<sup>48</sup> NPs

with a diameter smaller than 50 nm exhibit higher uptake as compared to larger NPs.<sup>49</sup> An 808-nm laser with a power density of 1.77 W/cm<sup>2</sup> was used to irradiate the sample in the well plate for 20 min. Immediately after laser irradiation, the cells were treated with trypan blue and observed under a bright field microscope. The imaging results are shown in Fig. 2. The dotted line in Fig. 2a represents the laser boundary. The images clearly show that the cells in the laser exposed section of the endocytosed NPs have undergone necrosis and hence appear blue after staining, as compared to the unexposed part, in which most cells stayed transparent. The cell death can be primarily attributed to necrosis due to the dramatic temperature increase in the first 5 mins of laser exposure based on the illustration in Fig. 1c. The temperature eventually reached the hyperthermic region and resulted in cell membrane disruption,<sup>50, 51</sup> allowing the trypan blue to enter the necrotic cell.



**Fig. 2** Brightfield images (4 $\times$ ) of (a) caki-2 cells incubated with BBTEHT NPs in which partial area was illuminated by the laser for 20 mins. The demarcation shows laser exposed section of the cells which is stained blue due to necrosis. (b) and (d) Caki-2 cells incubated with BBTEHT NPs and Au nanorods respectively in which the entire well was illuminated by the laser for 20 mins. The concentrations of BBTEHT NPs and Au nanorods were both 35  $\mu$ g/mL. (c) Caki-2 cells incubated with BBTEHT NPs without laser illumination.

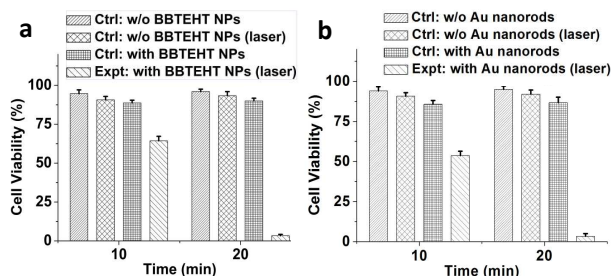


**Fig. 3** Photothermal destruction of caki-2 cells with or without BBTEHT NPs/ Au nanorods and NIR laser (808 nm, 1.77 W/cm<sup>2</sup>). (a) Cell viability after treatment using BBTEHT NPs with 10 and 20 mins of laser exposure. (b) Cell viability after treatment using Au nanorods with 10 and 20 mins of laser exposure. The concentrations of BBTEHT NPs and Au nanorods were both 35  $\mu$ g/mL.

To qualitatively evaluate the photothermal therapy effect of BBTEHT NPs as compared to Au nanorods, cells were separately incubated in a 96-well plate with PEGylated Au nanorods and BBTEHT NPs at equal concentrations (35  $\mu$ g/mL) using the same procedure. This time a smaller well size was used so that the 1.2 cm beam diameter of the laser could illuminate the entire well for better comparison of phototherapeutic efficacy of these two types of NPs. The results (Fig. 2b and 2d) show that cells with either BBTEHT NPs or Au nanorods induced nearly 100% necrosis in both of

which all cells were stained blue. The control cells without laser irradiation does not show any sign of necrosis. (Fig. 2c)

To further quantify the cell viability, the experimental group cells (incubated with BBTEHT NPs or nanorods and with laser illumination) were compared with three different control groups (without BBTEHT NPs or Au nanorods and without laser illumination, without BBTEHT NPs or Au nanorods but with laser illumination, and with BBTEHT NPs or Au nanorods but without laser illumination). In the experimental group, cells incubated with BBTEHT NPs for 6 h in a 96-well plate was exposed to the laser for 10 mins. At this time point, there was no apparent change in the viability of the three control groups. However, the experimental group at 10 mins showed almost 40 % dead cells as compared to the control groups (Fig. 3a). When the irradiation time was prolonged to 20 mins there were nearly no viable cells, resulting in close to 100% cell death in the experimental group (Fig. 3a). It can also be noticed that there were only slight changes in the cell viability in three control groups, signifying that there was no considerable cytotoxicity induced by NPs after 6 h of incubation. Similar results (Fig. 3b) were observed with PEGylated Au nanorods. These results suggest that BBTEHT NPs could be a good alternative to Au nanorods as the photothermal agent for cancer therapy.

## Conclusions

We have presented a novel photothermal therapeutic agent based on BBTEHT NPs with strong absorption in the NIR region. These NPs exhibit good colloidal stability, potentially higher photothermal conversion efficiency than that of commercial Au nanorods, and excellent photostability. Significant death of caki-2 cells was observed due to the hyperthermic effect, which was comparable to that of the Au nanorods both qualitatively and quantitatively. Although further *in vivo* study is needed to evaluate the performance in biodistribution and pharmacokinetics, BBTEHT NP can be a promising small-molecular organic photothermal agent, expected to be more biodegradable and clinically acceptable in comparison to other photothermal agents based on inorganic materials and conjugated polymers.

## Acknowledgments

M.W. is grateful to the funding support by a start-up grant from Nanyang Technological University, AcRF Tier 1 (M4011061.120, RG49/12) and AcRF Tier 2 (MOE2013-T2-1-059, ARC 36/13) from the Ministry of Education, Singapore. Q.L. acknowledges AcRF Tier 1 grant (RG38/14) from the Ministry of Education and ASTAR-ANR joint grant (102 167 0115) funded by ASTAR-SERC (Agency for Science Technology and Research, Science and Engineering Research Council) in Singapore. S.H. gratefully acknowledges the Ph.D. research scholarship from Nanyang Technological University.

## Notes and references

- <sup>a</sup> School of Chemical and Biomedical Engineering, Nanyang Technological University, 62 Nanyang Drive, Singapore 637459 E-mail: Q. Liu (quanliu@ntu.edu.sg); M. Wang (mfwang@ntu.edu.sg)  
<sup>†</sup> Electronic Supplementary Information (ESI) available: Experimental details, UV-vis spectra, SEM and TEM images of BBTEHT nanoparticles after laser irradiation. See DOI: 10.1039/c000000x/

1. J. T. Robinson, S. M. Tabakman, Y. Liang, H. Wang, H. S. Casalongue, D. Vinh and H. Dai, *J. Am. Chem. Soc.*, 2011, **133**, 6825-6831.
2. H. Liu, D. Chen, L. Li, T. Liu, L. Tan, X. Wu and F. Tang, *Angew. Chem. Int. Ed.*, 2011, **50**, 891-895.
3. S. Lal, S. E. Clare and N. J. Halas, *Acc. Chem. Res.*, 2008, **41**, 1842-1851.
4. D. Jaque, L. Martinez Maestro, B. Del Rosal, P. Haro-Gonzalez, A. Benayas, J. L. Plaza, E. Martin Rodriguez and J. Garcia Sole, *Nanoscale*, 2014, **6**, 9494-9530.
5. R. K. Kannadorai and Q. Liu, *Med. Phys.*, 2013, **40**, 103301.
6. H.-C. Huang, K. Rege and J. J. Heys, *ACS nano*, 2010, **4**, 2892-2900.
7. R. K. Kannadorai, G. G. Y. Chiew, K. Q. Luo and Q. Liu, *Cancer Letters*, 2015, **357**, 152-159.
8. E. Boisselier and D. Astruc, *Chem. Soc. Rev.*, 2009, **38**, 1759-1782.
9. L. Cheng, K. Yang, Y. Li, J. Chen, C. Wang, M. Shao, S. T. Lee and Z. Liu, *Angew. Chem. Int. Ed.*, 2011, **50**, 7385-7390.
10. W. Dong, Y. Li, D. Niu, Z. Ma, J. Gu, Y. Chen, W. Zhao, X. Liu, C. Liu and J. Shi, *Adv. Mater.*, 2011, **23**, 5392-5397.
11. Y. Xia, W. Li, C. M. Cobley, J. Chen, X. Xia, Q. Zhang, M. Yang, E. C. Cho and P. K. Brown, *Acc. Chem. Res.*, 2011, **44**, 914-924.
12. L. Dykman and N. Khlebtsov, *Chem. Soc. Rev.*, 2012, **41**, 2256-2282.
13. L. Nie, M. Chen, X. Sun, P. Rong, N. Zheng and X. Chen, *Nanoscale*, 2014, **6**, 1271-1276.
14. K. Yang, L. Feng, X. Shi and Z. Liu, *Chem. Soc. Rev.*, 2013, **42**, 530-547.
15. C. Li, S. Bolisetty, K. Chaitanya, J. Adamcik and R. Mezzenga, *Adv. Mater.*, 2013, **25**, 1010-1015.
16. U. Rocha, K. U. Kumar, C. Jacinto, I. Villa, F. Sanz-Rodriguez, C. Iglesias de la Cruz Mdel, A. Juarranz, E. Carrasco, F. C. van Veggel, E. Bovero, J. G. Sole and D. Jaque, *Small*, 2014, **10**, 1141-1154.
17. Q. Tian, M. Tang, Y. Sun, R. Zou, Z. Chen, M. Zhu, S. Yang, J. Wang, J. Wang and J. Hu, *Adv. Mater.*, 2011, **23**, 3542-3547.
18. Q. Tian, F. Jiang, R. Zou, Q. Liu, Z. Chen, M. Zhu, S. Yang, J. Wang, J. Wang and J. Hu, *ACS nano*, 2011, **5**, 9761-9771.
19. Z. Chen, Q. Wang, H. Wang, L. Zhang, G. Song, L. Song, J. Hu, H. Wang, J. Liu, M. Zhu and D. Zhao, *Adv. Mater.*, 2013, **25**, 2095-2100.
20. T. N. Lambert, N. L. Andrews, H. Gerung, T. J. Boyle, J. M. Oliver, B. S. Wilson and S. M. Han, *Small*, 2007, **3**, 691-699.
21. C. Lee, H. Kim, C. Hong, M. Kim, S. S. Hong, D. H. Lee and W. I. Lee, *J. Mater. Chem.*, 2008, **18**, 4790-4795.
22. S. Sharifi, S. Behzadi, S. Laurent, M. L. Forrest, P. Stroeve and M. Mahmoudi, *Chem. Soc. Rev.*, 2012, **41**, 2323-2343.
23. L. Cheng, K. Yang, Q. Chen and Z. Liu, *ACS nano*, 2012, **6**, 5605-5613.
24. Z. Zha, X. Yue, Q. Ren and Z. Dai, *Adv. Mater.*, 2013, **25**, 777-782.
25. Y. Liu, K. Ai, J. Liu, M. Deng, Y. He and L. Lu, *Adv. Mater.*, 2013, **25**, 1353-1359.
26. J. Yang, J. Choi, D. Bang, E. Kim, E. K. Lim, H. Park, J. S. Suh, K. Lee, K. H. Yoo, E. K. Kim, Y. M. Huh and S. Haam, *Angew. Chem. Int. Ed.*, 2011, **50**, 441-444.
27. L. Cheng, W. He, H. Gong, C. Wang, Q. Chen, Z. Cheng and Z. Liu, *Adv. Funct. Mater.*, 2013, **23**, 5893-5902.
28. M. Zheng, C. Yue, Y. Ma, P. Gong, P. Zhao, C. Zheng, Z. Sheng, P. Zhang, Z. Wang and L. Cai, *ACS nano*, 2013, **7**, 2056-2067.
29. X. He, X. Wu, K. Wang, B. Shi and L. Hai, *Biomaterials*, 2009, **30**, 5601-5609.
30. S. Zonghai, H. Dehong, X. Miaomiao, H. Meng, G. Ping and C. Lintao, *Nano-Micro Lett.*, 2013, **5**, 145-150.
31. C. S. Jin, J. F. Lovell, J. Chen and G. Zheng, *ACS nano*, 2013, **7**, 2541-2550.
32. G. Qian, B. Dai, M. Luo, D. Yu, J. Zhan, Z. Zhang, D. Ma and Z. Y. Wang, *Chem. Mater.*, 2008, **20**, 6208-6216.
33. J. Huber, C. Jung and S. Mecking, *Macromolecules*, 2012, **45**, 7799-7805.
34. J. D. Yuen, M. Wang, J. Fan, D. Sheberla, M. Kemei, N. Banerji, M. Scarongella, S. Valouch, T. Pho, R. Kumar, E. C. Chesnut, M. Bendikov and F. Wudl, *J. Polym. Sci., Part A: Polym. Chem.*, 2015, **53**, 287-293.
35. J. Fan, J. D. Yuen, M. Wang, J. Seifert, J.-H. Seo, A. R. Mohebbi, D. Zakhidov, A. Heeger and F. Wudl, *Adv. Mater.*, 2012, **24**, 2186-2190.
36. J. Fan, J. D. Yuen, W. Cui, J. Seifert, A. R. Mohebbi, M. Wang, H. Zhou, A. Heeger and F. Wudl, *Adv. Mater.*, 2012, **24**, 6164-6168.
37. T. T. Steckler, X. Zhang, J. Hwang, R. Honeyager, S. Ohira, X. H. Zhang, A. Grant, S. Ellinger, S. A. Odom, D. Sweat, D. B. Tanner, A. G. Rinzler, S. Barlow, J. L. Bredas, B. Kippelen, S. R. Marder and J. R. Reynolds, *J. Am. Chem. Soc.*, 2009, **131**, 2824-2826.
38. T. T. Steckler, K. A. Abboud, M. Craps, A. G. Rinzler and J. R. Reynolds, *Chem. Commun.*, 2007, 4904-4906.
39. A. Pitto-Barry and N. P. E. Barry, *Polym. Chem.*, 2014, **5**, 3291-3297.
40. A. V. Kabanov, E. V. Batrakova and V. Y. Alakhov, *J. Control. Release*, 2002, **82**, 189-212.
41. T. L. Tam, H. Li, F. Wei, K. J. Tan, C. Kloc, Y. M. Lam, S. G. Mhaisalkar and A. C. Grimsdale, *Org. Lett.*, 2010, **12**, 3340-3343.
42. S. Huang, S. Liu, K. Wang, C. Yang, Y. Luo, Y. Zhang, B. Cao, Y. Kang and M. Wang, *Nanoscale*, 2015, **7**, 889-895.
43. T. F. Cabada, C. S. L. de Pablo, A. M. Serrano, F. D. Guerrero, J. J. S. Olmedo and M. R. Gomez, *Int. J. Nanomedicine*, 2012, **7**, 1511-1523.
44. S. M. Shishido, A. B. Seabra, W. Loh and M. Ganzarolli de Oliveira, *Biomaterials*, 2003, **24**, 3543-3553.
45. P. Alexandridis and T. Alan Hatton, *Colloids Surf., A*, 1995, **96**, 1-46.
46. M. Malmsten, *Soft Matter*, 2006, **2**, 760-769.
47. S. Y. Lee, Y. Lee, J. E. Kim, T. G. Park and C.-H. Ahn, *J. Mater. Chem.*, 2009, **19**, 8198-8201.
48. S. Mukherjee, R. N. Ghosh and F. R. Maxfield, *Physiol. Rev.*, 1997, **77**, 759-803.
49. D. B. Chithrani, *Molec. Membrane Biol.*, 2010, **27**, 299-311.
50. B. V. Harmon, A. M. Corder, R. J. Collins, G. C. Gobé, J. Allen, D. J. Allan and J. F. R. Kerr, *Int. J. Rad. Biol.*, 1990, **58**, 845-858.
51. J. Zhou, X. Wang, L. Du, L. Zhao, F. Lei, W. Ouyang, Y. Zhang, Y. Liao and J. Tang, *Mol. Med. Rep.*, 2011, **4**, 187-191.